

## Sonogashira Coupling on an Extended Gold Surface in Vacuo: Reaction of Phenylacetylene with Iodobenzene on Au(111)

Vijay K. Kanuru, Georgios Kyriakou, Simon K. Beaumont,  
Anthoula C. Papageorgiou, David J. Watson,<sup>†</sup> and Richard M. Lambert\*

Department of Chemistry, University of Cambridge, Cambridge CB2 1EW, United Kingdom

Received February 8, 2010; E-mail: rml1@cam.ac.uk

**Abstract:** Temperature-programmed reaction measurements supported by scanning tunneling microscopy have shown that phenylacetylene and iodobenzene react on smooth Au(111) under vacuum conditions to yield biphenyl and diphenyldiacetylene, the result of homocoupling of the reactant molecules. They also produce *diphenylacetylene*, the result of Sonogashira cross-coupling, prototypical of a class of reactions that are of paramount importance in synthetic organic chemistry and whose mechanism remains controversial. Roughened Au(111) is completely inert toward all three reactions, indicating that the availability of crystallographically well-defined adsorption sites is crucially important. High-resolution X-ray photoelectron spectroscopy and near-edge X-ray absorption fine structure spectroscopy show that the reactants are initially present as intact, essentially flat-lying molecules and that the temperature threshold for Sonogashira coupling coincides with that for C–I bond scission in the iodobenzene reactant. The fractional-order kinetics and low temperature associated with desorption of the Sonogashira product suggest that the reaction occurs at the boundaries of islands of adsorbed reactants and that its appearance in the gas phase is rate-limited by the surface reaction. These findings demonstrate unambiguously and for the first time that this heterogeneous cross-coupling chemistry is an intrinsic property of extended, metallic pure gold surfaces: no other species, including solvent molecules, basic or charged (ionic) species are necessary to mediate the process.

### Introduction

The metal-catalyzed Sonogashira, Heck, and Suzuki coupling reactions that lead to the formation of new carbon–carbon bonds<sup>1–4</sup> are of major importance in synthetic organic chemistry. Often, metal nanoparticles are used as the source of catalytic material,<sup>5–7</sup> although it is a matter of continuing debate as to whether the active sites are present at the nanoparticle surfaces or reside in solution as molecular species leached from the solid phase.<sup>5,7–9</sup>

This remains a controversial issue, not least in the case of Sonogashira coupling.<sup>1,4,5,7</sup> Even though a very large number of investigations have been carried out, few of these have directly addressed the identity of the catalytically active species;

not infrequently, it is tacitly assumed or otherwise inferred that the reaction occurs homogeneously. In part, this reflects the difficulty of carrying out unambiguous analytical measurements that could provide an answer, and of course it is always possible that the extent to which homogeneous and heterogeneous pathways contribute may vary from case to case. Suffice it to say that evidence has been presented in favor of both points of view.<sup>5,7,10–12</sup> In the case of Pd, catalysis by leached species has been demonstrated,<sup>13,14</sup> whereas for other metals, the issue is more complex.<sup>15</sup> Using supported gold nanoparticles, González-Arellano et al.<sup>12</sup> reported leaching under the reaction conditions but took the view that the catalysis was heterogeneous; they also found no significant solvent effects.

Here we report on the interaction of phenylacetylene (PA) and iodobenzene (IB), prototypical of Sonogashira coupling, on an extended Au(111) surface under conditions of ultra high vacuum (UHV), where there is no possibility of homogeneous

<sup>†</sup> Present address: Department of Chemistry, University of Reading, Whiteknights, Reading RG6 6AD, United Kingdom.

(1) Chinchilla, R.; Nájera, C. *Chem. Rev.* **2007**, *107*, 874–922.

(2) Yin, L.; Liebscher, J. *Chem. Rev.* **2007**, *107*, 133–173.

(3) Hartwig, J. F. *Nature* **2008**, *455*, 314–322.

(4) Plenio, H. *Angew. Chem., Int. Ed.* **2008**, *47*, 6954–6956.

(5) Durand, J.; Teuma, E.; Gómez, M. *Eur. J. Inorg. Chem.* **2008**, 3577–3586.

(6) de Souza, R. O. M. A.; Bittar, M. S.; Mendes, L. V. P.; da Silva, C. M. F.; da Silva, V. T.; Antunes, O. A. C. *Synlett* **2008**, 1777–1780.

(7) Thathagar, M. B.; ten Elshof, J. E.; Rothenberg, G. *Angew. Chem., Int. Ed.* **2006**, *45*, 2886–2890.

(8) Widegren, J. A.; Finke, R. G. *J. Mol. Catal. A: Chem.* **2003**, *198*, 317–341.

(9) Phan, N. T. S.; van der Sluys, M.; Jones, C. W. *Adv. Synth. Catal.* **2006**, *348*, 609–679.

(10) Köhler, K.; Kleist, W.; Pröckl, S. S. *Inorg. Chem.* **2007**, *46*, 1876–1883.

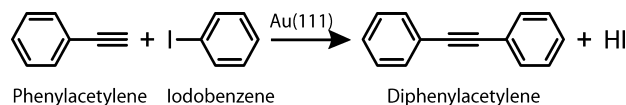
(11) Kanuru, V. K.; Humphrey, S. M.; Kyffin, J. M. W.; Jefferson, D. A.; Burton, J. W.; Armbrüster, M.; Lambert, R. M. *Dalton Trans.* **2009**, 7602–7605.

(12) González-Arellano, C.; Abad, A.; Corma, A.; García, H.; Iglesias, M.; Sánchez, F. *Angew. Chem., Int. Ed.* **2007**, *46*, 1536–1538.

(13) Gaikwad, A. V.; Holuigue, A.; Thathagar, M. B.; ten Elshof, J. E.; Rothenberg, G. *Chem.—Eur. J.* **2007**, *13*, 6908–6913.

(14) Thathagar, M. B.; Kooyman, P. J.; Boerleider, R.; Jansen, E.; Elsevier, C. J.; Rothenberg, G. *Adv. Synth. Catal.* **2005**, *347*, 1965–1968.

(15) Durán Pachón, L.; Rothenberg, G. *Appl. Organomet. Chem.* **2008**, *22*, 288–299.

**Scheme 1.** Sonogashira Coupling of Phenylacetylene and Iodobenzene

chemistry and the overall reaction may be written formally as shown in Scheme 1. Gold was chosen in view of current interest in this metal as a catalyst for an ever-widening range of organic reactions.<sup>16</sup>

By means of temperature-programmed reaction (TPR), scanning tunneling microscopy (STM), high-resolution synchrotron fast X-ray photoelectron spectroscopy (XPS), and near-edge X-ray absorption fine structure (NEXAFS) spectroscopy, it was found that the reactant molecules are adsorbed intact, lie flat, and in addition to undergoing homocoupling, Sonogashira cross-coupling to yield diphenylacetylene *does* occur with extreme sensitivity to the morphology of the gold surface.

### Experimental Methods

TPR experiments were conducted in Cambridge in a UHV chamber operated at a base pressure of  $1 \times 10^{-10}$  Torr. Reagent-grade phenylacetylene (98%, Sigma-Aldrich) and iodobenzene (99%, Fluka) were dosed onto the sample by backfilling the chamber, which was equipped with an Omicron 3 grid retarding field analyzer for low-energy electron diffraction (LEED)/Auger electron spectroscopy (AES) analysis and a VG 300 quadrupole mass spectrometer whose ionizer was positioned 5 mm from the front face of the sample. The Au(111) single crystal (10 mm  $\times$  15 mm  $\times$  1.0 mm) could be cooled to 100 K and heated to 1200 K; the temperature was monitored using a T1T2 thermocouple attached directly to the sample. The TPR heating ramp used was 4 K s<sup>-1</sup>, and the data presented here have been corrected for mass spectrometer sensitivity and molecular ionization cross sections. STM experiments were carried out in Cambridge using an Omicron variable-temperature UHV scanning tunneling microscope, which was operated in constant-current mode using etched tungsten tips.

High-resolution XPS and NEXAFS measurements were carried out on the SuperESCA beamline at the ELETTRA synchrotron radiation source in Trieste, Italy. Spectra were collected using a single-pass 32-channel concentric hemispherical electron analyzer. The excitation energies used for the acquisition of the C 1s, I 3d, and Au 4f spectra were 380, 720, and 180 eV, respectively. The angle between the analyzer entrance lens and the incoming photon beam was 70° in the horizontal plane. The Au(111) crystal was attached to a motorized manipulator via a tantalum back-plate fitted with a T1T2 thermocouple and could be heated resistively to 900 K or cooled to 90 K.

The Au(111) sample was cleaned by repeated cycles of Ar<sup>+</sup> sputtering (99.999%, Messer) followed by annealing at 550 K until a clean, atomically flat surface was obtained, as monitored by XPS and LEED (Trieste) or LEED and AES or STM (Cambridge). Quoted coverages for NEXAFS and XPS are based on estimation of the monolayer (ML) point from the associated shift in the C 1s binding energy that is apparent in the high-resolution XPS data for uptakes of each molecule and from the appearance of a multilayer peak in the thermal desorption data.

### Results and Discussion

First, we present reaction data obtained using smooth and deliberately roughened Au(111) surfaces. We then provide and

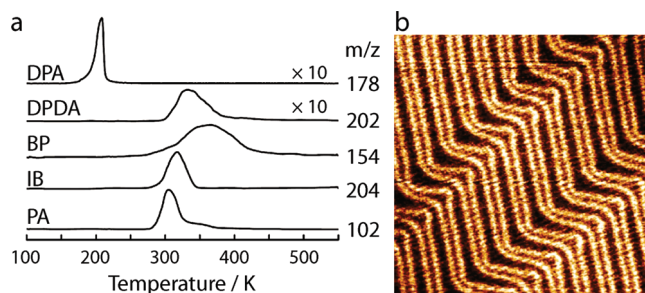
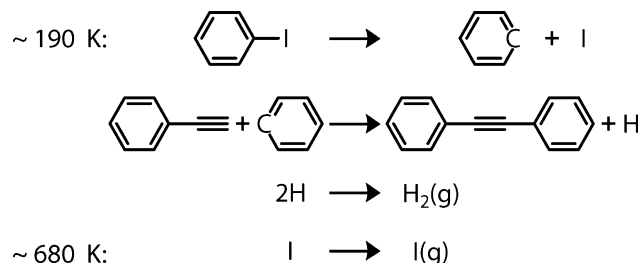


**Figure 1.** (a) TPR spectra of the reactants PA and IB and the products diphenylacetylene (DPA), diphenyldiacetylene (DPDA), and biphenyl (BP) after adsorption of 0.55 ML of IB + 0.25 ML of PA on Au(111) at 90 K. (b) Typical STM image of clean Au(111) surface showing the herringbone reconstruction (65 nm  $\times$  65 nm,  $V_{\text{gap}} = 2.41$  V,  $I = 0.21$  nA).

**Scheme 2.** Sonogashira Coupling in Vacuum on Au(111) (All Species Adsorbed unless Otherwise Indicated)



analyze corresponding NEXAFS and fast XPS data and discuss the reaction results in the light of these.

**Temperature-Programmed Reaction Measurements.** Figure 1a shows typical TPR spectra obtained after dosing 0.55 ML of IB and 0.25 ML of PA onto the smooth clean Au(111) surface (Figure 1b) at 90 K. The only gaseous organic products observed were (i) the Sonogashira cross-coupling product diphenylacetylene ( $m/z$  178) at  $\sim 200$  K and (ii) the two homocoupling products diphenyldiacetylene ( $m/z$  202) at  $\sim 330$  K and biphenyl ( $m/z$  154) at  $\sim 390$  K. Unreacted PA ( $m/z$  102) and IB ( $m/z$  204) desorbed at  $\sim 300$  and  $\sim 310$  K, respectively.<sup>17</sup> Notably, these results were obtained in the absence of any basic species (e.g., tetrabutylammonium acetate or  $\text{K}_2\text{CO}_3$ ), which are invariably employed when Sonogashira coupling is carried out under practical conditions in solution. The diphenylacetylene peak shape is characteristic of fractional-order kinetics,<sup>18</sup> suggesting that under our conditions, Sonogashira coupling takes place at the boundaries of islands of one or both reactants. Its low temperature indicates that the rate of appearance of gaseous diphenylacetylene is limited by a surface reaction.<sup>19</sup> The peak shapes of the homocoupling products diphenyldiacetylene and biphenyl are quite different from that of diphenylacetylene and are consistent with self-reaction of PA and IB either within islands or within a dispersed phase. In order to aid the discussion that follows, Scheme 2 shows a simple reaction scheme that is consistent with our findings.

An estimate of the reaction selectivity toward the Sonogashira product, diphenylacetylene, was carried out by calibrating the quadrupole mass spectrometer (allowing for mass discrimination

(16) (a) He, L.; Wang, L.-C.; Sun, H.; Ni, J.; Cao, Y.; He, H.-Y.; Fan, K.-N. *Angew. Chem., Int. Ed.* **2009**, *48*, 9538–9541. (b) Fujitani, T.; Nakamura, I.; Akita, T.; Okumura, M.; Haruta, M. *Angew. Chem., Int. Ed.* **2009**, *48*, 9515–9518. (c) Raptis, C.; Garcia, H.; Stratakis, M. *Angew. Chem., Int. Ed.* **2009**, *48*, 3133–3136. (d) Zhang, G.; Peng, Y.; Cui, L.; Zhang, L. *Angew. Chem., Int. Ed.* **2009**, *48*, 3112–3115.

(17) National Institute of Standards and Technology. NIST Chemistry WebBook. <http://webbook.nist.gov> (accessed Jan 10, 2010).

(18) Wu, H.-J.; Hsu, H.-K.; Chiang, C.-M. *J. Am. Chem. Soc.* **1999**, *121*, 4433–4442.

(19) Woodruff, D. P.; Delchar, T. A. *Modern Techniques of Surface Science*, 2nd ed.; Cambridge University Press: Cambridge, U.K., 1994; pp 375–377.

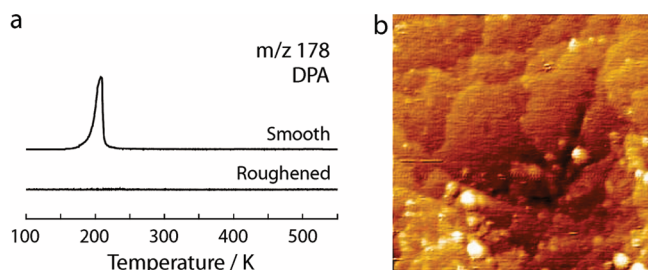


**Figure 2.** (a) Diphenylacetylene (DPA,  $m/z$  178) TPR spectra after dosing 0.55 ML of IB + 0.25 ML of PA on smooth and roughened Au(111) surfaces. (b) STM image of the roughened Au(111) surface (65 nm  $\times$  65 nm,  $V_{\text{gap}} = -1.00$  V,  $I = 0.87$  nA).

effects characteristic of these instruments) and correcting for ionization gauge sensitivities (see the Supporting Information). This procedure gave a lower limit of at least  $\sim 10\%$  for the selectivity toward diphenylacetylene formation. The selectivity toward Hay coupling was similarly estimated as  $\sim 10\%$ , the conversion of iodobenzene being  $\sim 60\%$ . Although relatively modest, the Sonogashira selectivity is on the order of reported selectivities for the same reaction carried out *in solution and in the presence of base*, catalyzed by supported Au nanoparticles. Basic species are known to promote Sonogashira reactions,<sup>20</sup> possibly by facilitating abstraction of the weakly acidic hydrogen atom on the alkyne.

How fast is this chemistry? It was not possible to specify a turnover frequency (TOF) in the normally understood sense, since in a one-shot TPR experiment there is no incident flux of reactant molecules, so the system is neither isothermal nor in a steady state. However, subject to certain assumptions (see the Supporting Information), one may obtain for a kind of pseudo-TOF a lower limit of  $\sim 30$  h<sup>-1</sup>, which is in the range of values reported for coupling reactions catalyzed by organometallic complexes.

As shown below by the XPS results, iodine was retained on the surface immediately after reaction, as indeed expected, given the strength of iodine chemisorption on gold. It could subsequently be desorbed (activation energy  $\approx 180$  kJ mol<sup>-1</sup>) at  $\sim 680$  K; the corresponding desorption data are shown in the Supporting Information. HI desorption was not detected, nor was it expected on thermodynamic grounds (see the Supporting Information). Hydrogen, the remaining possible product, was not detected because of its low yield and limited instrumental sensitivity at low  $m/z$ , exacerbated by the presence of the very small background hydrogen partial pressure that is always present in stainless steel UHV systems.

Figure 2 illustrates the morphology and reactive behavior toward Sonogashira coupling of the deliberately roughened surface (Ar<sup>+</sup>, 1 keV, 8.0  $\mu$ A, 90 min, no annealing) using the same reactant doses as for the smooth surface. It is evident that diphenylacetylene formation was totally quenched, as was that of the homocoupling products biphenyl and diphenyldiacetylene (not shown). A small amount of reactant desorption occurred, accompanied by extensive decomposition (as measured by XPS). Clearly, coupling reactions on gold are very sensitive to the details of surface structure. The inactivity of the rough Au surface may be due to unavailability of well-defined crystal facets of sufficient size. It may also be the case that the presence

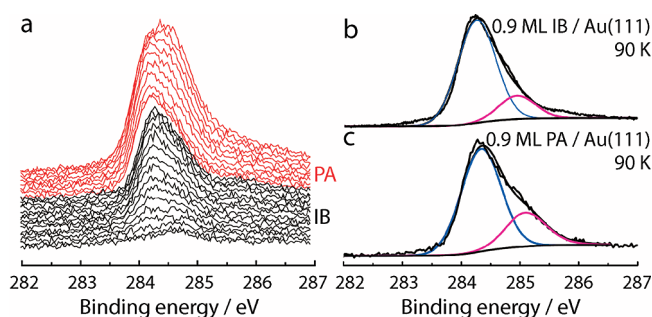


**Figure 3.** (a) Temperature dependence of C 1s spectra resulting from exposure of Au(111) to  $\sim 0.5$  ML of IB followed by  $\sim 0.5$  ML of PA at 90 K. (b) C 1s spectrum of 0.9 ML of IB. (c) C 1s spectrum of 0.9 ML of PA.

of low-coordinate Au sites on the roughened surface causes decomposition of the adsorbed reactants.

These findings demonstrate unambiguously that PA and IB undergo Sonogashira coupling on a well-ordered extended gold surface in vacuum. They also show that the reaction efficiency is sensitive to the details of surface structure, as only smooth surfaces with well-developed crystal planes were effective under our conditions. This observation suggests that metal particle size effects are likely to be significant when Sonogashira coupling of these reactants is carried out in solution in the presence of Au nanoparticles. Specifically, large particles should be more effective catalysts than small ones, *if* the reaction occurs heterogeneously.

**High-Resolution XPS.** Figure 3a shows C 1s XP spectra acquired during the uptake of  $\sim 0.5$  ML of IB followed by  $\sim 0.5$  ML of PA at 90 K. The IB spectrum is characterized by a major component at 284.3 eV associated with the phenyl ring and a smaller feature at 285.0 eV due to the carbon atom bonded to iodine. These features are more clearly apparent in Figure 3b, which shows the C 1s spectrum from 0.9 ML of IB at 90 K. The relative intensity of the two components was  $\sim 1:5$ , which is consistent with nondissociative adsorption of IB, a conclusion that was confirmed by the I 3d<sub>5/2</sub> spectra discussed below. Addition of  $\sim 0.5$  ML of PA to the 0.5 ML of IB resulted in the composite spectra shown in the upper part of Figure 3a. The principal component at  $\sim 284.3$  eV was increased in intensity and broadened, and its apparent binding energy was slightly downshifted. A broad feature at a binding energy of  $\sim 285.0$  eV also appeared, most likely due to the alkyne group. Interpretation was made possible by the results shown in Figure 3c, which refer to  $\sim 0.9$  ML of pure PA. Two components are present with an intensity ratio of  $\sim 2:6$ , again consistent with nondissociative molecular adsorption. The identical binding energy of 284.3 eV observed for the two molecules in the coadsorbed spectra (Figure 3a) and in the submonolayer spectra of the pure reactants (Figure 3b,c) confirms that when coadsorbed at a total coverage of  $\sim 1$  ML, both PA and IB were in contact with the Au(111) surface, as multilayer adsorption would have resulted in a measurable shift to higher binding energy if this were not the case.

Figure 4a,b shows subsets of the C 1s and I 3d data acquired in a separate experiment in which a mixed adsorbed layer ( $\sim 1$  ML) of IB and PA was annealed at 5 K min<sup>-1</sup>. In this case, an amount of PA was initially present in a second layer, resulting in the C 1s high-energy shoulder at  $\sim 284.7$  eV; it had disappeared by 173 K, resulting in a downshift of the C 1s emission maximum by 0.3 eV. The corresponding I 3d<sub>5/2,3/2</sub> spectrum increased in intensity as a result of desorption of the

(20) Thathagar, M. B.; Beckers, J.; Rothenberg, G. *Green Chem.* **2004**, 6, 215–218.



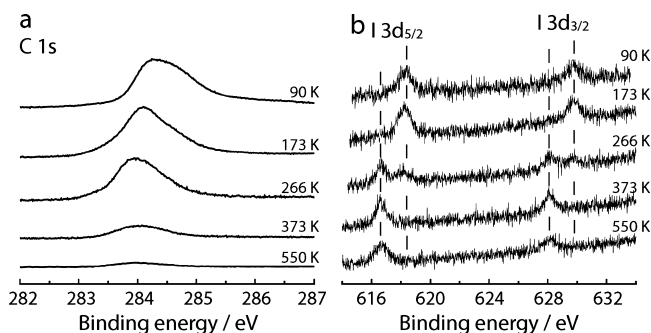


**Figure 4.** (a) Time- and temperature-dependent C 1s spectra resulting from annealing a mixed layer of  $\sim 0.5$  ML of IB + 0.7 ML pf PA at  $5 \text{ K min}^{-1}$ . (b) Corresponding I 3d spectra.

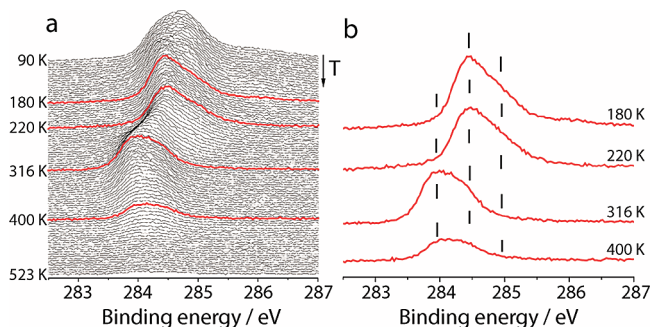


**Figure 5.** (a) Time and temperature dependence of the C 1s spectrum, commencing with multilayers of IB adsorbed at 90 K. (b) Data subset extracted from (a).

overlying PA multilayer, and the observed binding energies correspond to organically bound iodine ( $\text{I } 3d_{5/2} = 618.4 \text{ eV}$ ). A further increase in temperature to 266 K shifted the C 1s envelope to lower binding energy, consistent with scission of the C–I bond in IB; this process is analogous to oxidative addition of an organic halide to an organometallic complex, as noted by Celio et al.<sup>21</sup> This conclusion was strongly confirmed by the corresponding iodine spectrum, which exhibited emission due to two chemically distinct forms of I: the original component at 618.4 eV and a new feature shifted to lower binding energy by 1.7 eV, as expected for  $\text{I}_{\text{ads}}$  resulting from C–I bond scission,<sup>22</sup> a process that was complete by  $\sim 373 \text{ K}$ . Notably, the onset of IB dissociation ( $\sim 266 \text{ K}$ ) corresponds well with the onset of Sonogashira coupling observed in the Cambridge TPR experiments (Figure 1). Additionally, the overall loss of C 1s intensity between 266 and 373 K agrees with the desorption of unreacted IB and PA as well as the biphenyl product, as shown in Figure 1. The residual C 1s peak at 373 K centered at  $\sim 284.0 \text{ eV}$  was almost certainly due to biphenyl, as will be shown, this was confirmed by the NEXAFS results.

In view of the above results and the fact that it seemed at least plausible for Sonogashira coupling to be preceded by C–I scission in IB, it was of interest to examine the latter process in more detail by means of the C 1s spectrum. Figure 5a shows the time and temperature dependence of the C 1s spectrum starting with a multilayer of pure IB; a subset of these data is presented in Figure 5b. Between 90 and 180 K, the main C 1s component shifted from 284.7 to 284.4 eV, indicative of multilayer desorption. Between 180 and 220 K, there was no

significant shift. Between 220 and 316 K, a progressive downshift of the C 1s intensity maximum to lower binding energies occurred, accompanied by loss of the characteristic shoulder at 284.9 eV corresponding to scission of the C–I bond. This more accurate result corroborates the temperature dependence of the iodine spectra observed for the mixed IB + PA layer. Specifically, the C 1s data show that the threshold for C–I scission in IB is  $\sim 220 \text{ K}$ , in very good agreement with the temperature regime over which the Sonogashira cross-coupling product was observed in the TPR measurements (Figure 1). In this connection, Syomin and Koel<sup>23</sup> studied the adsorption and reaction of IB on Au(111) by temperature-programmed desorption and IR reflection absorption spectroscopy (IRAS) and also found that scission of the C–I bond takes place at 200–250 K, resulting in immediate formation of biphenyl. The latter observation is of relevance in the present case, as it suggests an explanation for the relatively limited Sonogashira selectivity found here: in the absence of base, which serves to activate PA, phenyl species resulting from C–I scission tend to undergo homocoupling to yield biphenyl before they can be captured by PA to yield the Sonogashira product. This effect would presumably be accentuated if the IB molecules tended to form islands, as reported for IB on Cu(110),<sup>24</sup> and indeed, we found that biphenyl was the main product in the TPR experiments (Figure 1).

**NEXAFS Spectroscopy of Individual Reactants, Coadsorbed Reactants, and the Reaction.** NEXAFS measurements were carried out on IB and PA adsorbed separately or coadsorbed and as a function of temperature. Figure 6a shows C K-edge NEXAFS spectra of 0.5 ML of PA on Au(111) at 90 K recorded at five photon incidence angles ( $\theta$ , defined relative to the surface plane). Prominent resonances due to  $\text{C } 1s \rightarrow \pi^*$  and  $\text{C } 1s \rightarrow \sigma^*$  transitions are apparent, and a summary of the assignments and associated transitions is given in Table 1.

Resonances A and B at 285.0 and 285.7 eV correspond to  $\text{C } 1s \rightarrow \pi^*$  transitions and are crucial for estimating the orientation of PA on Au(111): Figure 6b clarifies the different  $\theta$  dependences of resonances A (phenyl group) and B (alkyne group, which contains  $\pi_x$  and  $\pi_y$  components that exhibit opposite angular variation and therefore no net change). It is noteworthy that the C K-edge NEXAFS spectrum of gaseous PA<sup>25,26</sup> exhibits a clear and characteristic splitting of the  $\text{C } 1s \rightarrow \pi^*$  resonance at  $\sim 285.5 \text{ eV}$  that results from conjugation of the alkyne and phenyl groups in the molecule. To a first approximation, the lower-energy resonance may be considered as phenyl-like, while that at higher energy includes contributions from both the phenyl and alkyne groups. This splitting disappears upon adsorption of PA on Cu and Pt surfaces<sup>26,28</sup> because of appreciable rehybridization of the molecular orbitals of the alkyne group, which adopts a distorted  $\text{sp}^2$  configuration. However in the present case, the characteristic split of the  $\text{C } 1s \rightarrow \pi^*$  resonance is still apparent, indicating preservation of the molecular geometry and consistent with the XPS results. Five

(21) Celio, H.; Smith, K. C.; White, J. M. *J. Am. Chem. Soc.* **1999**, *121*, 10422–10423.

(22) Bugyi, L.; Oszkó, A.; Solymosi, F. *Surf. Sci.* **2003**, *539*, 1–13.

(23) Syomin, D.; Koel, B. E. *Surf. Sci.* **2001**, *490*, 265–273.

(24) Dougherty, D. B.; Lee, J.; Yates, J. T., Jr. *J. Phys. Chem. B* **2006**, *110*, 20077–20080.

(25) Carravetta, V.; Polzonetti, G.; Iucci, G.; Russo, M. V.; Paolucci, G.; Barnaba, M. *Chem. Phys. Lett.* **1998**, *288*, 37–46.

(26) Polzonetti, G.; Carravetta, V.; Russo, M. V.; Contini, G.; Parent, P.; Laffon, C. *J. Electron Spectrosc. Relat. Phenom.* **1999**, *98*, 175–187.

(27) Iucci, G.; Carravetta, V.; Paolucci, G.; Goldoni, A.; Russo, M. V.; Polzonetti, G. *Chem. Phys.* **2005**, *310*, 43–49.

(28) Iucci, G.; Carravetta, V.; Altamura, P.; Russo, M. V.; Paolucci, G.; Goldoni, A.; Polzonetti, G. *Chem. Phys.* **2004**, *302*, 43–52.

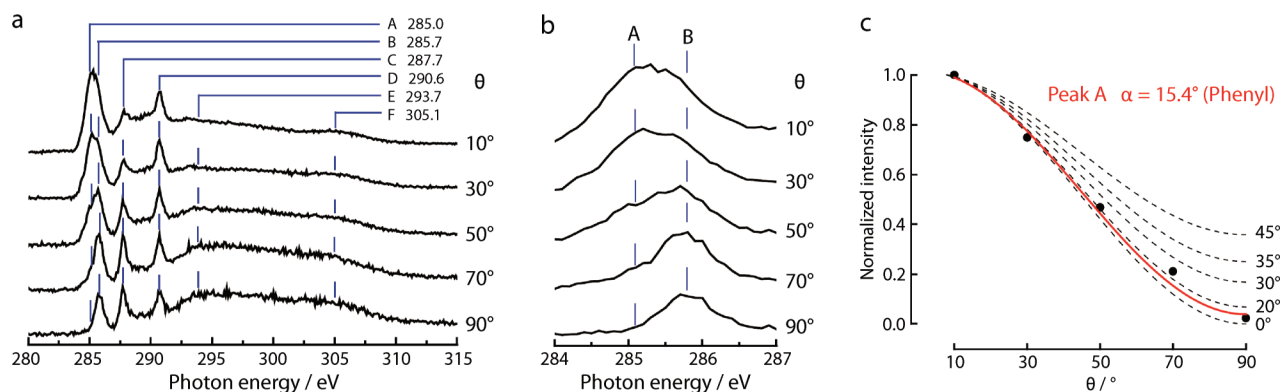


**Figure 6.** (a) C K-edge NEXAFS spectra acquired at five photon incidence angles  $\theta$  for a  $\sim 0.5$  ML coverage of PA on Au(111) at 90 K. (b) Expanded scale for the leading  $\pi^*$  resonances A and B. (c) Curve-fitting analysis of the  $\theta$  dependence of  $\pi^*$  resonance A to estimate the phenyl ring tilt angle,  $\alpha$ .

**Table 1.** Resonance Assignments for the C K-Edge NEXAFS of PA on Au(111)<sup>25–28</sup>

peak	energy (eV)	assignment
A	285.0	C1s $\rightarrow \pi^*$ (phenyl) PA
B	285.7	C1s $\rightarrow \pi^*$ (alkyne) PA
C	287.7	C1s $\rightarrow \sigma^*$ C–H
D	290.6	C1s $\rightarrow \pi^*b_{2g} + \sigma^*$ C–H
E	293.7	C1s $\rightarrow \sigma^*$ C–C
F	305.1	C1s $\rightarrow \sigma^*$ C–C

**Table 2.** Resonance Assignments for C K-Edge NEXAFS of IB on Au(111)<sup>30,31</sup>

peak	energy (eV)	assignment
A	285.1	C1s $\rightarrow \pi^*$ phenyl
B	285.8	C1s $\rightarrow \pi^*$ phenyl
C	287.7	C1s $\rightarrow \sigma^*$ C–H
D	288.8	C1s $\rightarrow \pi^*b_{2g}$
E	290.6	C1s $\rightarrow \sigma^*$ C–H
F	293.5	C1s $\rightarrow \sigma^*$ C–C
G	305.3	C1s $\rightarrow \sigma^*$ C–C

more transitions are resolved at higher photon energies, assigned in Table 1, but not required for analysis.<sup>25–28</sup>

The angular dependence of C 1s  $\rightarrow \pi^*$  resonance A provides a means of determining the orientation of the molecules with respect to the surface.<sup>29</sup> Figure 6c shows the observed normalized intensities overlaid with a series of theoretical curves,<sup>29</sup> with the best least-squares fit yielding a tilt angle ( $\alpha$ ) of  $15^\circ$  with an uncertainty of  $5^\circ$  for the orientation of the phenyl group with respect to the surface (i.e., the molecule lies almost flat).

Similarly, Figure 7a shows C K-edge NEXAFS spectra for 0.5 ML of IB acquired at five photon incidence angles. Seven resonances were resolved, and their assignment is summarized in Table 2. The first two resonances at 285.1 and 286.0 eV are assigned to the C 1s  $\rightarrow \pi^*$  transition, which is split into two components by the presence of the hetero-

atom as a result of the reduction in symmetry from  $D_{6h}$  to  $C_{2v}$ ,<sup>30,31</sup> as is more clearly apparent in Figure 7b. This splitting provides strong confirmation that adsorption of IB at 90 K is nondissociative, again in good accord with the XPS data. At higher photon energies, five more transitions were clearly resolved and can be assigned (Table 2).

The angular dependence of resonance A at 285.1 eV was used to calculate the orientation of IB with respect to the surface as before,<sup>29</sup> and the results are shown in Figure 7c: IB also adsorbs relatively flat on the surface ( $\alpha = 15^\circ$ ), which agrees well with the observations of Syomin and Koel,<sup>23</sup> who used IRAS to show that at submonolayer coverages, IB adsorbs almost flat on Au(111).

Finally, we used NEXAFS in an attempt to examine coadsorption of PA and IB at 90 K and the subsequent reaction and

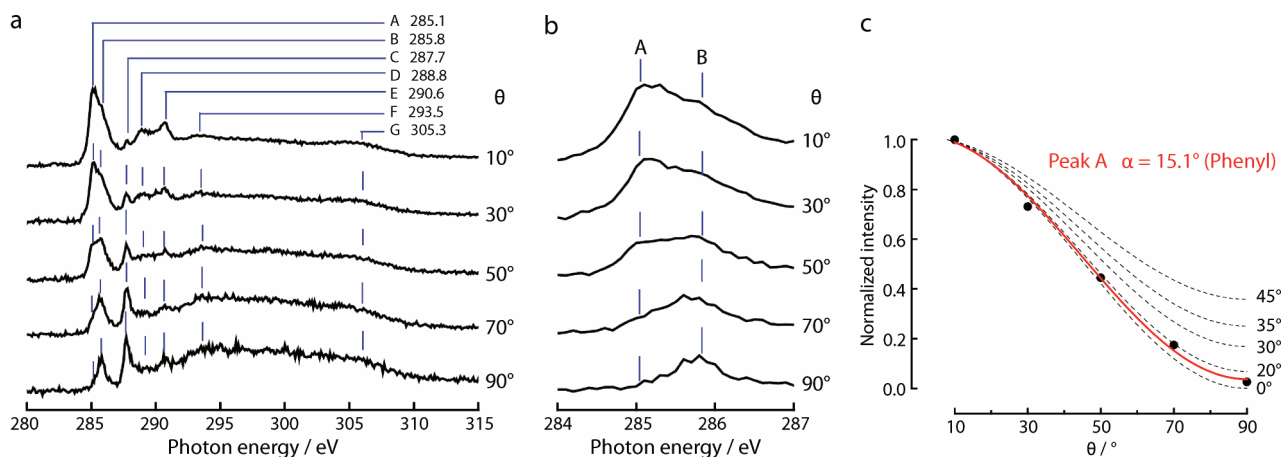


**Figure 7.** (a) C K-edge NEXAFS spectra acquired at five photon incidence angles  $\theta$  for a  $\sim 0.5$  ML coverage of IB on Au(111). (b) Close up of principal  $\pi^*$  resonances A and B. (c) Curve-fitting analysis of the photon-angle dependence of  $\pi^*$  resonance A to estimate the corresponding phenyl ring tilt angle,  $\alpha$ .

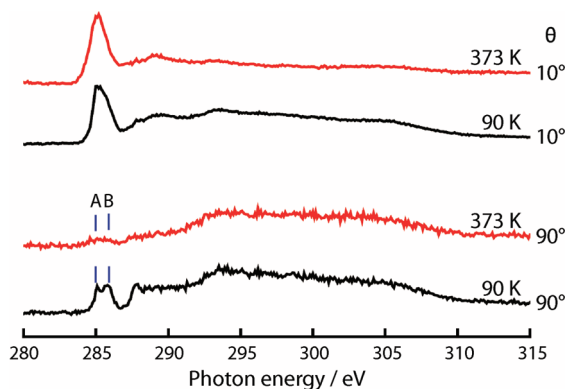


**Figure 8.** C K-edge NEXAFS spectra acquired at photon incidence angles  $\theta$  of 10 and 90° for the coadsorption of  $\sim 0.5$  ML of IB and  $\sim 0.7$  ML of PA on Au(111) at 90 K followed by annealing to 373 K.

evolution of the mixed layer with increasing temperature. Beam time limitations allowed acquisition of data at only two temperatures, 90 and 373 K, as shown in Figure 8. At 90 K, the superposition of resonances and possible masking of some resonances by a contribution from a partial multilayer<sup>32,33</sup> makes the identification of these features unreliable. However, according to the TPR results (Figure 1), the only species surviving on the surface at 373 K should have been the reaction product biphenyl, and indeed, this fits well with the single resonance observed at that temperature. Analysis of this feature as a function of photon incidence angle (see the Supporting Information) gave a tilt angle of  $\sim 0^\circ$ . That is, biphenyl lies absolutely flat, as might be expected.<sup>23</sup>

## Conclusions

In summary, phenylacetylene and iodobenzene react on smooth Au(111) under vacuum conditions to yield the homocoupling products diphenyldiacetylene and biphenyl and, with appreciable selectivity, diphenylacetylene, the product of Sonogashira cross-coupling and the process of paramount interest in this work. These findings provide the first unambiguous demonstration that this heterogeneous cross-coupling chemistry is an intrinsic property of extended, metallic pure gold surfaces. The minimum necessary and sufficient conditions are coadsorbed reactants on a clean, well-ordered gold surface; no other species, including charged (ionic) species are necessary to mediate the process. Roughened Au(111) is completely inactive toward all three reactions, indicating that the availability of crystallographically well-defined adsorption sites is crucially important. In view of the many reported correlations between single-crystal reaction data and nanoparticle catalysis at the

gas–solid interface (e.g., see the reviews by Ertl and Freund<sup>34</sup> and Somorjai et al.<sup>35</sup>), it seems possible that pronounced particle-size effects may arise when these coupling reactions are catalyzed by gold nanoparticles under practical conditions. Indeed, Besson et al.<sup>36</sup> have reported superior catalytic performance for larger Pt nanoparticles in solution in comparison with smaller ones. High-resolution XPS and NEXAFS spectroscopy have demonstrated that the reactants are initially present as intact, essentially flat-lying molecules. The temperature threshold for Sonogashira coupling coincides with that for C–I bond scission in iodobenzene, although this does not prove that C–I bond scission is the reaction-initiating step. The fractional-order kinetics and low temperature associated with desorption of the Sonogashira product suggest that under our conditions it is formed at the boundaries of islands of adsorbed reactants and that its appearance in the gas phase is rate-limited by a surface reaction.

**Acknowledgment.** The authors thank Silvano Lizzit, Sandra Gardonio, and Michele Tranquillin for their assistance during the synchrotron experiments. V.K.K. acknowledges the award of a Gates Cambridge Scholarship. G.K. and A.C.P. acknowledge financial support from the U.K. Engineering and Physical Sciences Research Council. S.K.B. acknowledges financial support from Cambridge University; Trinity Hall, Cambridge; the U.K. Society of the Chemical Industry; and the International Precious Metals Institute.

**Supporting Information Available:** Experimental methodology and calibration procedure used for estimating reaction selectivity; angle-resolved C K-edge NEXAFS spectra of the biphenyl homocoupling product at 373 K; iodine desorption spectrum; thermochemistry of  $H_2$  versus HI desorption; thermochemistry of I atom versus  $I_2$  molecule desorption; and pseudo-TOF estimation. This material is available free of charge via the Internet at <http://pubs.acs.org>.

JA1011542

- (29) Stöhr, J.; Outka, D. A. *Phys. Rev. B* **1987**, *36*, 7891–7905.
- (30) Yang, M. X.; Xi, M.; Yuan, H.; Bent, B. E.; Stevens, P.; White, J. M. *Surf. Sci.* **1995**, *341*, 9–18.
- (31) Lee, A. F.; Chang, Z.; Hackett, S. F. J.; Newman, A. D.; Wilson, K. *J. Phys. Chem. C* **2007**, *111*, 10455–10460.
- (32) Solomon, J. L.; Madix, R. J.; Stöhr, J. *Surf. Sci.* **1991**, *255*, 12–30.
- (33) Kong, M. J.; Teplyakov, A. V.; Lyubovitsky, J. G.; Bent, S. F. *Surf. Sci.* **1998**, *411*, 286–293.
- (34) Ertl, G.; Freund, H.-J. *Phys. Today* **1999**, *52*, 32–38.
- (35) Somorjai, G. A.; Frei, H.; Park, J. Y. *J. Am. Chem. Soc.* **2009**, *131*, 16589–16605.
- (36) Besson, C.; Finney, E. E.; Finke, R. G. *Chem. Mater.* **2005**, *17*, 4925–4938.